不等厚 ULC-BH钢激光拼焊接头硬化机制

倪加明, 李铸国, 蔡 艳, 吴毅雄
(上海交通大学 上海市激光制造与材料改性重点实验室, 上海 200240)


倪加明

摘 要: 采用两种激光光斑加热位置, 对不等厚超低碳烘烤硬化钢板进行激光拼焊, 分别测定拼焊接头的显微硬度, 对比分析其组织性能差异, 探讨热影响区硬化软化机制. 结果表明, 光斑偏向厚板时, 拼焊焊缝两侧组织硬度曲线较为对称; 在焊接热循环作用下, 热影响区基体中饱和科特雷尔(Cottrell)气团析出细小弥散的 NbC等第二相颗粒, 使得热影响区强硬化; 光斑置中时, 容易使薄板热输入过渡, 析出的第二相颗粒聚集长大, 热影响区重新软化, 容易导致冲压时开裂.

关键词: 激光拼焊; 超低碳烘烤硬化钢; 显微硬度; 不等厚
中图分类号: TG456.7 文献标识码: A 文章编号: 0253-360X(2010)08-0017-04

0 序 言

激光拼焊广泛应用于汽车车身覆盖件和结构组件工业生产, 是汽车车身轻量化(ultra light steel auto body, ULSAB)的重要技术组成[1]. 激光拼焊可以将不同厚度、强度及表面镀层状况的钢板缝合成冲压毛坯件, 降低车身自重, 降低能源消耗, 减少尾气排放, 改善车身防撞性能[2,3]. 激光制造拥有高度自动化和系统集成化, 有益于提升生产效率, 降低长期生产成本, 作为环境友好型的先进工业制造技术大量研究.

不等厚超低碳烘烤硬化钢 (ultra low carbon bake hardening steel, ULC-BH) 激光拼焊板焊缝质量好, 拥有如前所述的优点, 但仍存在部分不足有待改善. 激光拼焊 ULC-BH钢焊缝硬度较高, 容易造成应力集中; 靠近焊缝的薄板热影响区容易过热软化, 导致冲压成形时开裂, 相比均匀厚度钢板, 冲压成形性能下降. 诸多研究采用模拟改进冲压成形以适应激光拼焊板的成形性能[4,5]. 激光拼焊 ULC-BH钢的热影响区烘烤硬化性因素则考虑较少.

针对不等厚激光拼焊, 变化激光加热光斑位置, 调节厚板和薄板焊接热输入, 测定接头显微硬度分布, 分析光斑位置对焊缝两侧热影响区组织和性能影响, 探讨激光拼焊热影响区硬化及过时效机制.

收稿日期: 2009-03-16
基金项目: 国家科技部国际科技合作基金资助项目(2006DFA52680); 上海市科委国际合作基金资助项目(061107030)

1 试验方法

试验材料为高强度的超低碳钢烘烤硬化汽车用钢板, 厚度分别为 1 mm与 1.5 mm. 化学成分如表 1所示, 此类钢板具有较好的成形性能. 采用高功率连续 CO_2激光为热源, 激光束垂直入射, 激光光束焦点光斑直径约为 0.75 mm, 选取厚板上表面为焊接时激光束焦平面, 分别采用光斑置于对接中线和偏向厚板侧 0.2 mm进行焊接, 如图 1所示.

表 1 超低碳烘烤硬化钢的化学成分(质量分数, %)
Table 1 Chemical composition of ULC-BH steel

C	Mn	P	S	Al	Nb	Fe
0.0035	0.11	0.007	0.007	0.035	0.058	余量

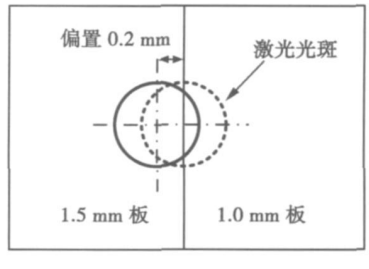

图 1 激光光斑偏置补偿示意图
Fig. 1 Schematic diagram of different laser spot position offset

为分析不等厚激光拼焊钢板接头组织和性能, 观察接头截面宏观形貌, 并测量接头截面显微硬度

曲线. 采用金相显微镜和扫描电子显微镜分析接头微观组织, 参照已有烘烤硬化机制, 分析激光焊接过程 ULC-BH钢接头热影响区硬化和过时效软化.

2 试验结果

2.1 焊缝成形

激光拼焊薄板时热输入小, 焊接速度快, 拼焊的焊缝和热影响区相对于普通焊接均要小. 然而, 激光拼焊大比率不等厚板时, 两侧板材厚度差异大, 两侧钢板散热性能及母材熔化吸收能量差异, 导致激光焊缝两侧热影响区的组织和力学性能不均. 为了尽量使焊缝两侧组织性能相近, 采取激光光斑偏置厚板措施, 以补偿厚度导致的焊接热输入的需求差异. 不同光斑位置所用焊接参数: 激光光斑偏置厚板 0.2 mm时, 激光功率为 5.3 kW, 焊接速度为 2 m/min; 激光光斑置中时, 激光功率为 5.5 kW, 焊接速度为 2 m/min. 置中时熔化厚板光斑面积变小, 所需激光功率增加. 所得接头截面形貌如图 2所示.

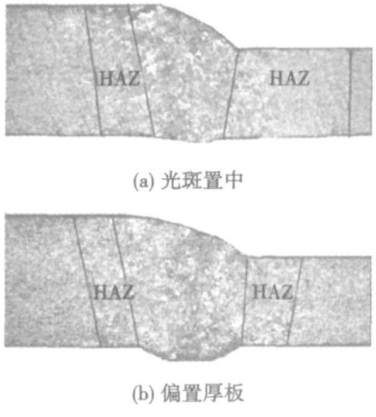

图 2 不同光斑位置所得接头截面形貌对比

Fig. 2 Comparison of cross-sections of welded joints with different laser spot position offsets

光斑偏置时薄板的热影响区宽度比光斑置中时小很多, 薄厚接头过渡平缓. 说明采用激光光斑偏置厚板, 配比不等厚度两侧板材的激光能量输入, 恰当增多厚板能量输入以满足熔化需要, 同时减少薄板激光能量输入, 减轻焊接对其过热影响. 是平衡处理两侧不等厚钢板焊接热输入的有效手段.

2.2 显微硬度

材料的显微硬度能一定程度表征材料强度等力学性能. 为考察激光光斑偏置对焊缝性能影响, 分别测定接头截面显微硬度曲线, 测量直线位置为距底部 0.5 mm的薄板中心线. 所得结果绘成曲线如图 3所示, 焊缝组织硬度值均高于母材, 厚板靠近焊缝的热影响区硬度高达 160 HV. 光斑偏置时, 显微硬度曲线在焊缝两侧分布较为对称. 光斑置中时, 显微硬度曲线在两侧热影响区分布没有对称性, 薄板热影响区存在相当宽范围的硬度下降. 分析认为, 光斑置中时, 为满足厚板熔化热需求, 容易致使薄板过热. 与此不同, 基于不等厚两侧散热能力和熔化热量差异考虑, 采用激光光斑偏置厚板措施, 有利于平衡两侧热需求, 获得的不等厚接头两侧组织性能较为对称.

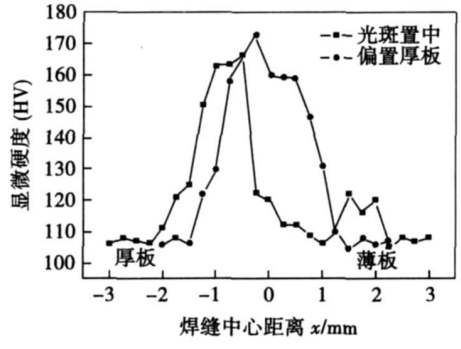

图 3 显微硬度曲线对比

Fig. 3 Microhardness comparison of cross-sections of welded joint with different laser spot position offsets

2.3 显微组织

为了研究不等厚激光拼焊板光斑置中时薄板热影响区硬度降低原因, 对其焊缝显微组织进行分析. 各区域组织如图 4所示, 原始母材为轧制获得的晶粒均匀铁素体组织, 平均晶粒尺寸为 16 μm; 焊缝金属为形态较为复杂的准多边形铁素体组织; 焊缝两侧热影响区组织也为准多边形铁素体组织, 薄板热影响粗晶区的平均晶粒尺寸为 38 μm, 厚板粗晶晶粒尺寸与之相近为 36 μm. 然而, 薄板过热而产生大量粗晶粒, 热影响粗晶区大, 而厚板热影响粗晶区小. 图 5所示为扫描电子显微镜观察到的薄板热影响粗晶区和母材组织. 薄板热影响粗晶区的多边形铁素体基体上有大量细小的第二相颗粒析出, 而母材铁素体晶粒内没有发现第二相颗粒, 第二相颗粒析出是热影响区组织硬化和软化的重要因素.

3 讨 论

3.1 热影响区硬化微观机制

烘烤硬化钢板母材为晶粒大小均匀的铁素体, 铁素体基体内固溶有大量 C原子. 室温下, 原本固

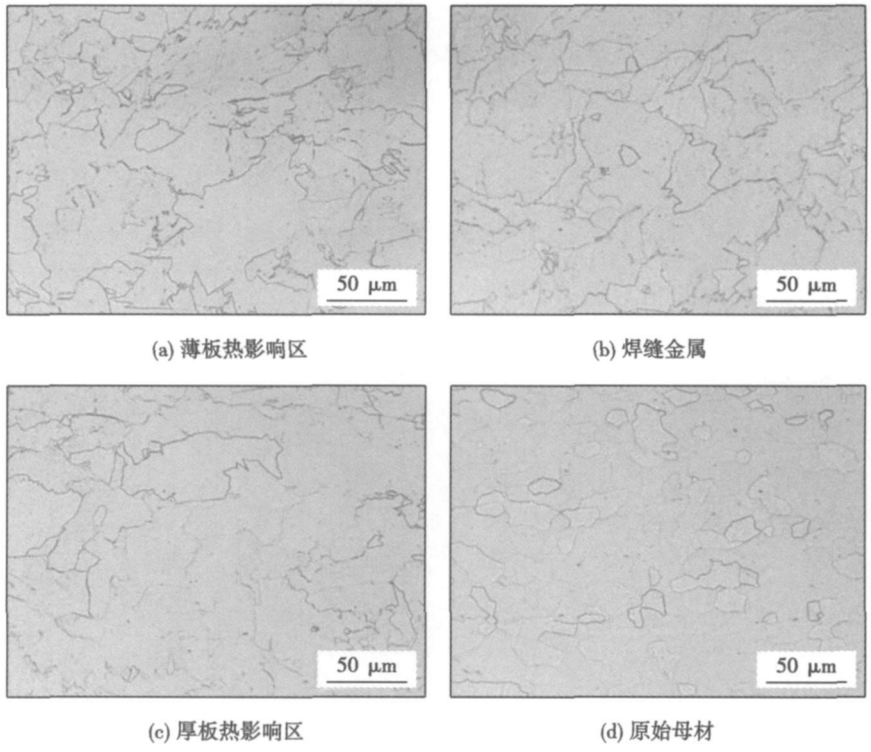

(a) 薄板热影响区　(b) 焊缝金属

(c) 厚板热影响区　(d) 原始母材

图 4　激光拼焊焊缝显微组织

Fig. 4　Microstructure of laser welded joint

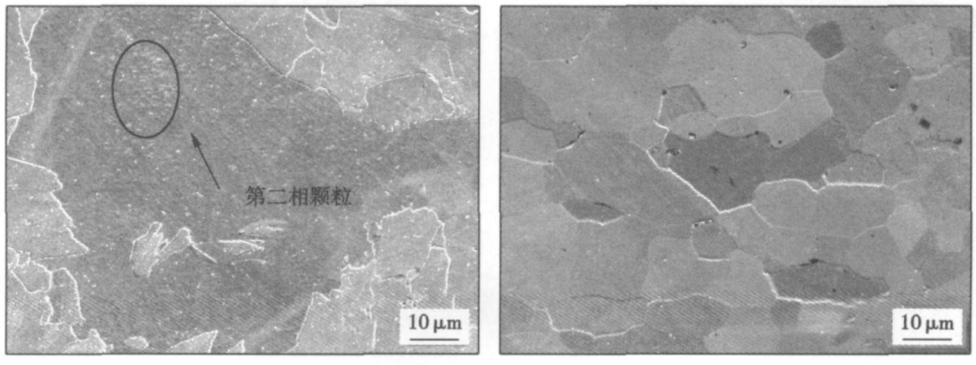

(a) 粗晶组织　(b) 母材组织

图 5　热影响区硬化微观组织对比

Fig. 5　Microstructure comparison of HAZ before and after heating

溶于基体的 C原子缓慢向位错等缺陷扩散. 激光焊接时,热影响区受热输入和应力应变的双重作用. 应力应变作用下,热影响区位错密度迅速增加,固溶于基体的 C原子向位错扩散距离缩短. 同时,随热影响区温度升高, C原子扩散激活能增加,向位错扩散速度加快,最终 C原子钉扎位错,形成 Cottrel气团,阻碍位错运动,使热影响区硬度增加. 是烘烤硬化钢的高温应变时效性初级阶段. 随时效时间延长,进入高温应变时效第二阶段,饱和的 Cottrel气团将析出细小的 NbC第二相颗粒. 热影响区由于大量细小弥散的第二相质点从基体中析出,强度和硬度大幅提升. 偏置厚板焊接时,热影响区硬度由焊前的 110 HV增至焊后的 160 HV,根据德国 DIN50150标准换算,其抗拉强度增加 160 MPa.

3.2　热影响区重新软化微观机制

激光光斑置中焊接时,往往致使薄板热输入过大,扩散激活能迅速增加,同时高温时间延长,导致热影响区析出的第二相颗粒大量聚集析出,反而使其硬度下降,属于高温过时效. 根据第二相颗粒与滑移位错的交互作用机制,同一尺寸第二相在尺寸很小且与基体保持较好的共格关系时属于位错切过机制,其强度增量随颗粒尺寸增加而增加;而当其尺

寸增大并与基体的共格关系遭受破坏时属于奥罗万（Orowan）机制，其强化作用随颗粒尺寸增加而递减[6]．钢铁材料临界转化尺寸 d_c 可由以下公式计算，即

$$\frac{d_c}{\ln\left(\frac{d_c}{2b}\right)}=0.209\frac{Gb^2}{K\gamma} \tag{1}$$

式中：G为切变弹性模量；b为位错柏格斯矢量的绝对值；γ为第二相与基体的界面能．以析出 NbC第二相颗粒为例，参照钢铁材料相关数据，根据式（1），计算的铁素体基体中 NbC颗粒的临界转换尺寸约为 1.6 nm[6]．过热薄板的粗晶区内第二相颗粒尺寸为几十纳米，远大于此数值，故对位错阻碍作用减弱，热影响区硬度降低．

4 结 论

（1）激光光斑置中时，不等厚拼焊板焊缝两侧硬度分布不对称，薄板热影响区硬度降低；光斑偏置厚板 0.2 mm时，焊缝两侧组织的硬度曲线较为对称．

（2）光斑偏置厚板 0.2 mm时，焊缝和热影响区为准多边形铁素体组织．焊接热循环作用下，饱和 Cottrell气团析出细小弥散的 NbC等第二相颗粒，焊缝和热影响区强硬化．

（3）光斑置中时，薄板热影响区容易热输入过多，导致第二相颗粒聚集长大，按照 Orowan机制其强化作用减弱，热影响区硬度和强度下降，容易在后续冲压过程开裂．

参考文献：

[1] Palletta R J, Lark R J. The use of tailored blanks in the manufacture of construction components[J]. Journal of Materials Processing Technology, 2001, 117(1-2): 249-254.

[2] Krizan D, Waterschoot T, Koruk A, et al. Bake hardening of laser welded dual phase steel[J]. Steel Research International, 2003, 74(10): 639-645.

[3] 余淑荣，樊 丁，熊进辉．异厚度铝合金薄板激光拼焊应力应变场数值模拟[J]．焊接学报，2008，29(10)：25-28.
Yu Shurong, Fan Ding, Xiong Jinhui. Numerical simulation on stress-strain field of laser welding aluminum alloy joints with different thickness[J]. Transactions of the China Welding Institution, 2008, 29(10): 25-28.

[4] Gaied S, Roelandt J M, Pinard F, et al. Experimental and numerical assessment of Tailor Welded Blanks formability[J]. Journal of Materials Processing Technology, 2009, 209(1): 387-395.

[5] 姜银方，张永康，朱元右，等．差厚激光拼焊板焊缝移动与回弹控制[J]．焊接学报，2008，29(1)：31-35.
Jiang Yinfang, Zhang Yongkang, Zhu Yuanyou, et al. Investigation of springback control and movement of welding seam of tailor-welded blanks in forming with blank holder force[J]. Transactions of the China Welding Institution, 2008, 29(1): 31-35.

[6] 雍歧龙．钢铁材料中的第二相[M]．北京：冶金工业出版社，2006.

作者简介：倪加明，男，1983年出生，博士研究生．从事激光焊接方面研究工作．发表论文 3篇．

Email: njm@sjtu.edu.cn

MAIN TOPICS, ABSTRACTS & KEYWORDS

precipitated from the saturated Cottrell atmospheres of bake hardening steel, which help to harden the HAZ. However, without offset more laser power is required to melt the thick sheet, but thin sheet also receives more power. Surplus heat input results in the obvious precipitate growth and the softening HAZ of the thin side sheet. Stamping cracking always occurs in the HAZ of the thin side sheet.

Key words: tailored bland laser welding; ultra low carbon bake hardening steel; microhardness; different thickness

Influence of current converting speed on 2219 aluminum alloy VPTIG weld joints ..... CONG Baoqiang, QI Bojin (School of Mechanical Engineering and Automation, Beihang University, Beijing 100191, China). p. 21—24

Abstract: A novel arc welding technique with ultrafast convert variable polarity square-waveform for aluminum alloys was developed. The influence of variable polarity current converting speed on the porosity and mechanical properties of 2219-T87 weld was studied based on the conventional and ultrafast-convert variable polarity tungsten inert gas (VPTIG) welding techniques, respectively. The experimental results show that compared with the conventional variable polarity welding, weld porosity is obviously improved in the case of the faster current converting speed and less zero-crossing time. The number of gas pore is reduced and eliminated indeed. The tensile strength and percentage elongation of the weld joints are respectively enhanced by 8.97% and 12.6% due to the softening of weld bond area.

Key words: high strength aluminum alloy; ultrafast convert variable polarity; weld porosity

Thermal damage analysis of vacuum brazing diamond with Ni-Cr alloy ..... LU Jinbin[+2], TANG Feng, MENG Pu, WANG Zhixin[+1] (1. College of Materials & Chemical Engineering, Zhongyuan University of Technology, Zhengzhou 450007, China; 2. College of Mechanical Engineering, Nanjing University of Aeronautics and Astronautics, Nanjing 210016, China). p. 25—28

Abstract: Brazing diamond tools has the characteristics of high protrude and strong bonding, which will be significantly degraded in brazing with the excessively high temperature, and so the thermal damage for the diamond was analyzed. The diamond was brazed in vacuum by using Ni-Cr alloy, then the surface of sample was observed by SEM and EDS, and the heat stress and graphitization on the surface were detected with Laser Raman spectroscopy. The results show that more carbide, such as Cr_3C_2, Cr_7C_3, exists on the diamond surface, and a little graphitization and chemical soakage take place on the surface. The tensile stress in the top of diamond is 110 MPa, and the compressive stress in the bottom of diamond is 520 MPa.

Key words: vacuum brazing; diamond; Ni-Cr alloy; thermal damage

Ultrasonic residual stress measurement of 300 km/h high-speed train body ..... LU Hao[+2], MA Zifei, LIU Xuesong, FANG Hongyuan[+1] (1. State Key Laboratory of Advanced Welding Production Technology, Harbin Institute of Technology, Harbin 150001, China; 2. Welding Laboratory, CSR Qingdao Sifang Locomotive and Rolling Stock Co., Ltd., Qingdao 266111, China). p. 29—32

Abstract: Aluminum alloy is used to make the high-speed train body. Because the bearing pressure of the body is large, the residual stress distribution is urgently needs to measurement. Based on the acoustoelasticity, the residual stress can be measured by ultrasonic method. Ultrasonic stress measurement experimental installation is established with critically refracted longitudinal wave. The residual stress of high-speed train body structure is measured by the system. The safety evaluation virtual model of welded structure concept is proposed.

Key words: ultrasonic; welding residual stress; high speed train

Joining test of telerobotic welding rapid tool changing interface ..... DONG Na, LI Haichao, CHEN Youquan, GAO Hongming, WU Lin[+1] (1. State Key Laboratory of Advanced Welding Production Technology, Harbin Institute of Technology, Harbin 150001, China; 2. Department of Mechanical Engineering, Armor Technique Institute of PLA, Changchun 130117, China). p. 33—36

Abstract: According to the equipment maintenance in dangerous environment, the remote welding robot has to prepare much more than the welding task for the welding and process after welding. Rapid tool changing interface meets the requirement of kinds of tools changing in the remote maintenance, which improves the generability of the remote welding robot but enhances the complexity of teleoperation. So the practical application key of rapid tool changing interface is feasibility verification of interface joining operation. The testing environment is composed of the video feedback, force feedback, teleoperation joy stick and human-robot interface etc. According to the feedback information, the tool joining was tele-handled by the control mode of tele-teaching. The teleoperation time and the changing of the force and force moment was recorded. Results show that the rapid tool changing interface is competent in the tool joining task.

Key words: remote welding robot; rapid tool changing interface; tele-teaching; force feedback

Laser butt welding of TNi shape memory alloy sheet ..... CHEN Yuhua, KE Liming, HUANG Yongde, XU Shilong (National Defense Key Disciplines Laboratory of Light Alloy Processing Science and Technology, Nanchang Hangkong University, Nanchang 330063, China). p. 37—40

Abstract: The butt welding of 0.2 mm thick TNi shape memory alloy (SMA) sheet was carried out by using low power impulse laser, and the tensile strength, fracture strain, phase change process and shape memory effect of welded joint were studied. The results show that using low power impulse laser can realize good butt welding of TNi SMA sheet. The tensile strength of welded joint of cold rolled TNi SMA achieves 97% of base metal, and fracture strain achieves 95% of base metal. When the welded joint is annealed after welding, its tensile strength is